MOLECULAR AND CELLULAR BIOLOGY, Oct. 2005, p. 8703–8716 Vol. 25, No. 19
0270-7306/05/$08.00+0 doi:10.1128/MCB.25.19.8703–8716.2005

Control of Fetal Growth and Neonatal Survival by the RasGAP-Associated Endoribonuclease G3BP

Latifa Zekri,[1]† Karim Chebli,[1]† Hélène Tourrière,[1] Finn C. Nielsen,[2] Thomas V. O. Hansen,[2] Abdelhaq Rami,[3] and Jamal Tazi[1]*

Institut de Génétique Moléculaire de Montpellier UMR 5535, IFR 122, Centre National de Recherche Scientifique, 1919 Route de Mende, 34293 Montpellier, France[1]; Department of Clinical Biochemistry, University Hospital Rigshospitalet, University of Copenhagen, Copenhagen, Denmark[2]; and Anatomisches Institut III, Uniklinik, Theodor-Stern-Kai 7, 60590 Frankfurt/Main, Germany[3]

Received 6 April 2005/Returned for modification 6 May 2005/Accepted 6 July 2005

The regulation of mRNA stability plays a major role in the control of gene expression during cell proliferation, differentiation, and development. Here, we show that inactivation of the RasGAP-associated endoribonuclease (G3BP)-encoding gene leads to embryonic lethality and growth retardation. *G3BP*$^{-/-}$ mice that survived to term exhibited increased apoptotic cell death in the central nervous system and neonatal lethality. Both in mouse embryonic fibroblasts and during development, the absence of G3BP altered the expression of essential growth factors, among which imprinted gene products and growth arrest-specific mRNAs were outstanding. The results demonstrate that G3BP is essential for proper embryonic growth and development by mediating the coordinate expression of multiple imprinted growth-regulatory transcripts.

Control of mRNA decay plays a crucial role in the regulation of gene expression. This process relies on an equilibrium between ribonucleases and mRNA binding factors, which affect mRNA half-life in response to extracellular signals (57, 65). The half-lives of mammalian mRNAs range from minutes to days, and the stability of critical transcripts varies with the growth/differentiation status of the cell or in response to extracellular stimuli (4, 48). The mechanisms and regulation of mRNA degradation have been intensively studied over recent years (41). A small number of general pathways appear to be responsible for degrading most mRNAs, so regulatory mechanisms are thought to be targeted to the initial events that direct the mRNA into one of these pathways, maintain it in a translationally inactive state, or permit its translation (44). The three major decay-initiating events are deadenylation, endonucleolytic cleavage, and decapping (41). A growing number of mRNAs have been found to be degraded through endonucleolytic cleavage, including the mRNAs encoding the transferrin receptor (5), the cytokine gro-α (55), avian apo-very low density lipoprotein II (6), maternal homeodomain proteins (9), albumin (10, 42), insulin-like growth factor II (IGF-II) (35, 36, 37), c-*myc* (24, 32), and α-globin (63). However, the physiological function of this type of regulation is still largely unknown.

Genetic approaches have made it feasible to identify mRNases in lower organisms and to analyze the phenotypes of cells with mRNase gene mutations (18). In contrast, vertebrate cells with mRNase gene mutations have not been generated. This study focuses on a protein that associates with Ras GTPase-activating protein p120 (RasGAP) (21) (G3BP), which harbors an intrinsic endonuclease activity that cleaves in vitro the AU-rich element, a *cis*-acting element located in the 3′ untranslated regions (UTRs) of mouse and human c-*myc* mRNAs (59). G3BP, which has a predicted molecular mass of 52 kDa, comprises an amino (N)-terminal domain (residues 1 to 120) homologous to nuclear transporter factor 2 (NTF2) and a central domain rich in acidic residues (residues 140 to 240), followed by a carboxyl (C)-terminal RNA recognition module (RRM) (21). The RRM domain mediates the binding of G3BP to specific RNA sequences so G3BP can exert its function as a CA dinucleotide-specific single-strand-specific endoribonuclease (59).

The G3BP family includes two members in mammals, G3BP1 (referred to as G3BP) and G3BP2 (25, 29). G3BP1 and -2 are encoded by distinct genes on human chromosomes 5 and 4 and mouse chromosomes 11 and 5, respectively. In addition, the NTF2 domain, which is the most highly conserved domain in G3BPs, is found in other factors, including NTF2 itself and the highly related TAP, another RNA binding protein, and p15, which cooperatively function in nuclear mRNA export (56). Accordingly, the NTF2 domain of G3BP influences the cellular localization of the protein and its oligomerization with itself or with other partners (58). Recently, it has been shown that phosphorylation of G3BP at Ser-149, which is 20 amino acids C terminal to the NTF2-like domain, plays a key role in mediating protein-protein interactions and in controlling G3BP's subcellular localization (58, 59). One other interesting feature of G3BP is that both its phosphorylation and its association with RasGAP in the particulate fraction of cells are affected by extracellular stimuli, consistent with the possibility that G3BP plays a role in modulating the fate of mRNA via external signals.

Besides its cleaving activity, G3BP was also identified as DNA/RNA helicase VIII (62), as a regulator of the activity of ubiquitin protease (14, 51), or as a transcription cofactor dur-

* Corresponding author. Mailing address: Institut de Génétique Moléculaire de Montpellier UMR 5535, IFR 122, Centre National de Recherche Scientifique, 1919 route de Mende, 34293 Montpellier, France. Phone: 33 (0) 4 67 61 36 85. Fax: 33 (0) 4 67 04 02 45. E-mail: jamal.tazi@igmm.cnrs.fr.

† Latifa Zekri and Karim Chebli contributed equally to this work.

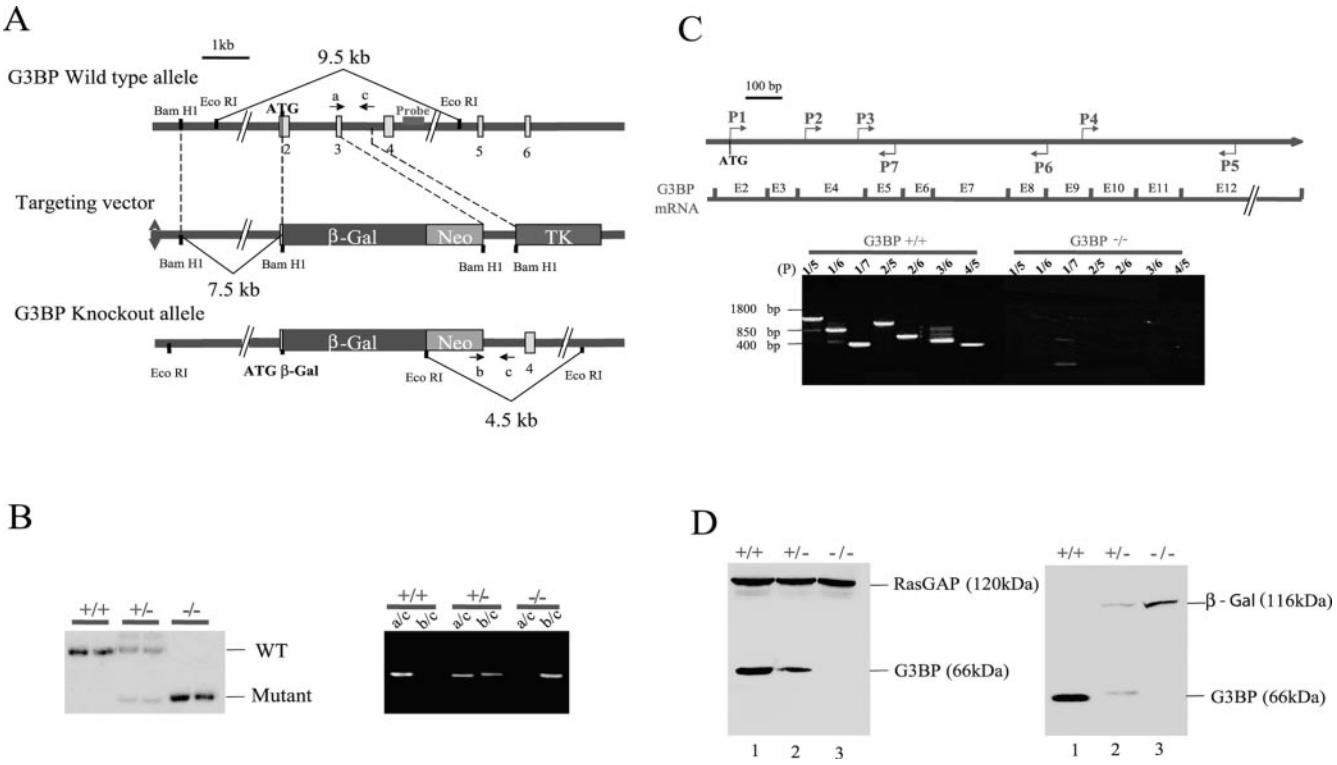

FIG. 1. Gene targeting of the *G3BP* locus. (A) Structure of the mouse *G3BP* locus, the targeting vector, and the targeted allele after homologous recombination. Restriction sites (BamHI) relevant to the targeting construct and the screening strategies are indicated. Neo, neomycin; TK, thymidine kinase. (B) Southern blot analysis of DNA from wild-type and G3BP mutant embryos (left). Genomic DNA was digested with EcoRI, and the blot was hybridized with the 3′ external probe shown in panel A. The bands representing the WT (9.5-kb) and mutant (4.5-kb) alleles are indicated. (Right) PCR analysis of tail DNA from $G3BP^{+/+}$, $G3BP^{+/-}$, and $G3BP^{-/-}$ E18.5 mice. The PCR primers (a, b, and c) used are shown in panel A. (C) Expression of the G3BP transcript in wild-type, $G3BP^{+/-}$, and $G3BP^{-/-}$ mice. RNAs from E18.5 embryos were examined for G3BP expression by multiplex RT-PCR with the indicated primers (P) for G3BP. The products were separated by agarose gel electrophoresis and visualized by ethidium bromide staining. (D) Western blot analysis of G3BP protein from E12.5 embryos. Total homogenates were prepared from each genotype as in panel B, and equal amounts of protein were analyzed by SDS-polyacrylamide gel electrophoresis, followed by immunoblotting with monoclonal anti-G3BP (1F1). As controls, immunoblotting with anti-p120 RasGAP (left) and monoclonal anti-β-galactosidase (right) was performed.

ing vaccinia virus late replication (28). However, different systems have been used to demonstrate these activities, and as a result, it is not clear whether all the activities are required for G3BP function(s) in vivo. As a first step toward determining the in vivo function(s) of G3BP, we have employed a gene deletion strategy in mice. We find that G3BP plays an important role during embryonic growth and at birth. Monitoring the global expression pattern, using Affymetrix oligonucleotide arrays, in isolated wild-type (WT) and G3BP knockout (KO) fibroblasts, we show that the expression of the growth arrest-specific genes and imprinted genes was specifically increased in the absence of G3BP. Importantly, G3BP KO mice were also characterized by altered expression of these genes during embryogenesis. Altogether, these findings offer substantial support to a model whereby G3BP integrates activating signals and silencing signals, quantitatively and dynamically, to control fetal growth and viability at birth.

MATERIALS AND METHODS

Construction of G3BP targeting vector. Genomic clones of *G3BP* were obtained by screening a mouse 129 Sv genomic λ library by standard techniques. A 7.5-kb BamHI G3BP genomic fragment located immediately upstream of the ATG translation start site was subcloned into the pBKS vector to obtain pBKS-G3BP 5′. A β-galactosidase (β-Gal) cassette was subcloned into pBKS-G3BP 5′, inserting the β-Gal ATG start site in place of the *G3BP* ATG start site, and a resistance cassette was placed in the transcriptional orientation opposite to that of the endogenous *G3BP* gene. A 0.7-kb BamHI genomic fragment downstream of exon 3 of *G3BP* was added. Our targeting vector also included a thymidine kinase cassette to allow enrichment of targeted embryonic stem (ES) cells with ganciclovir.

Generation of targeted ES cells and G3BP-deficient mice. The G3BP targeting vector was linearized with NotI and electroporated into mouse CK35 ES cells. Recombinant clones were selected in the presence of G418 (400 μg/ml) and ganciclovir (2 μM). Twenty-eight targeted ES clones were identified and verified by Southern blot hybridization of EcoRI-digested genomic DNA with an external probe, as indicated in Fig. 1B. The ES clones were injected into C57BL/6 blastocysts and gave rise to germ line-transmitting chimeric mice. Chimeric males were mated with 129 Sv females, and F_1 agouti pups were analyzed for the presence of the transgene by PCR analysis of tail genomic DNA with the following primers: TCTGACCTCCACAAGCATACCACTC (a), GGAAAGAAC TCTTCCTATGCCCACG (b), and CGCCTTCTTGACGAGTTCTTCTGAG (c) (Fig. 1B). Heterozygous $G3BP^{+/-}$ mice were crossed to obtain homozygous $G3BP^{-/-}$ mice. The strain was maintained in a 129 Sv background.

MEF preparation and cell signaling. $G3BP^{+/-}$ females were crossed with $G3BP^{+/-}$ males, and the embryos were dissected 14.5 days after the detection of vaginal plugs. The head and internal organs were removed, and the embryos were minced and incubated in trypsin for 30 min at 37°C. The cells were resuspended in Dulbecco's modified Eagle medium supplemented with 10% fetal calf serum, 50 U/ml penicillin, 50 μg/ml streptomycin, and 2 mM L-glutamine. Fetal livers and/or yolk sacs were used for PCR genotyping. For growth experiments,

mouse embryonic fibroblasts (MEFs) were plated at low density (2×10^3 cells/6-cm dish), and their growth rate was monitored by daily counting for 8 days. Cell cycle distribution was scored by staining asynchronous cells with propidium iodide, followed by BD Biosciences cytometer analysis.

To test whether the absence of G3BP affects Ras signaling pathways, MEFs were starved for 24 h and stimulated by serum for the indicated times. The cells were lysed in Laemmli loading buffer, and proteins were analyzed by Western blotting using a 1/1,000 dilution of primary antibodies against Akt, phospho-Akt, or phospho-Erk protein (BioLabs).

Analysis of G3BP transcript and protein. Total RNA prepared from embryonic day 18.5 (E18.5) wild-type and mutant embryos using Trizol reagent (Invitrogen) was treated with RNase-free DNase I. First-strand cDNA was generated with an F-S-cDNA synthesis kit (Amersham Biosciences) using an oligo(dT) primer. G3BP expression was analyzed by multiplex reverse transcription (RT)-PCR using several pairs of primers: GATGGTTATGGAGAAGC (P1), AAAC TTCACCAACTGCCACACCAAG (P2), TTGTCCTTGCTCCTGAG (P3), AT GGTGAGGCACCCTGACAGT (P4), CCTGGTTTCTGCACCATGCCTCC (P5), GGTTTAGATTCTGGACGGGGCTGTG (P6), and CCTGAGGCTCAG TGACAAACCCACC (P7). PCR products were separated by agarose gel electrophoresis and visualized by ethidium bromide staining (Fig. 1C).

Total protein extracts from $G3BP^{+/+}$, $G3BP^{+/-}$, and $G3BP^{-/-}$ embryos at different stages of development were homogenized in 1 ml of HNTG buffer as described previously (21) using lysing Matrix D (Q-BIOgene). All samples were quantified using bicinchoninic acid protein assay reagent (Pierce), and 30 μg of each sample was analyzed by Western blotting using dilutions of primary antibodies as follows: 1/3,000 for anti-G3BP (1F1), 1/500 for anti-RasGAP (GP200), and 1/40 for β-galactosidase (Oncogene Research Products) (Fig. 1D).

Statistical analysis and growth kinetics studies. Three types of crosses were studied: (i) between heterozygous mice, (ii) male $G3BP^{+/-}$ with female WT mice, and (iii) male WT with female $G3BP^{+/-}$ mice. For growth kinetics studies, crosses between heterozygous mice were done, and pregnant females were dissected at various embryonic stages (E0.5 was defined as the day of vaginal-plug detection). Embryos were weighed, and mutant animals were distinguished from the wild type by genotyping the corresponding yolk sacs.

Morphological and histological analyses. For morphological analysis, wild-type and $G3BP^{-/-}$ embryos at 10.5, 11.5, and 12.5 days postcoitum were washed two times in phosphate-buffered saline (PBS) (Sigma) and fixed overnight with 4% paraformaldehyde (PFA) in PBS at 4°C. After three washes in PBS, the embryos were stored at 4°C (Fig. 2).

For histological analysis, the indicated organs from caesarean pups at E18.5 were fixed in 10% buffered formalin (Sigma) and embedded in paraffin. Sections (5 μm) were stained with 1% celestine blue and 1% acid fuchsin. In the staining procedure used, pyknotic cells appeared bright red on examination under the light microscope, showed extensive cytorrhexis and/or karyorrhexis, and were readily distinguished from surviving cells. For evaluation of apoptotic cell death in brain tissues, immunostaining was performed using antibodies that recognize the active form of caspase 3, which is considered a specific marker of neuronal apoptosis.

Whole-mount RNA in situ hybridization. Embryos were fixed overnight in 4% PFA at 4°C. After three washes in PBT (PBS plus 1% Tween 20), the embryos were rehydrated in a series of methanol-PBT, bleached in 6% hydrogen peroxide, treated with 10 μg proteinase K (Roche) per ml for various times depending on the age of the embryo, and washed two times with 2 mg glycine per ml in PBT for 10 min. The embryos were then postfixed in 4% PFA-0.2% glutaraldehyde for 20 min, washed three times in PBT for 10 min, and prehybridized in hybridization buffer (50% formamide, 5× SSC, pH 5.0 [1× SSC is 0.15 M NaCl plus 0.015 M sodium citrate], 0.5% CHAPS {3-[(3-cholamidopropyl)-dimethylammonio]-1-propanesulfonate]}, 5 mM EDTA, 0.2% Tween 20, 1% sodium dodecyl sulfate [SDS], 100 μg/ml heparin [Sigma], 50 μg/ml yeast tRNA [Sigma]) at 65°C for 3 h. The embryos were then hybridized at 65°C overnight in hybridization buffer containing 1 μg/ml of IGF-II digoxigenin-labeled antisense riboprobe. After hybridization, the embryos were washed in hybridization buffer, in wash buffer I (50% formamide, 5× SSC, pH 5.0, 1% SDS), and in RNase buffer (0.5 M NaCl, 10 mM Tris-HCl, pH 7.5, 0.1% Tween 20) before they were treated with 20 μg RNase per ml at 37°C and washed in wash buffer II (50% formamide, 2× SSC, pH 5.0, and 1% SDS). Finally, the embryos were blocked in blocking buffer (1% sheep serum, 1% blocking reagent [Roche], 1.4 M NaCl, 27 mM KCl, 0.25 M Tris-HCl, pH 7.5, 1% Tween 20), and the transcripts were detected by overnight incubation at 4°C with anti-digoxigenin antibody (Roche) and nitroblue tetrazolium–5-bromo-4-chloro-3-indolylphosphate (Roche) staining as recommended by the manufacturer.

DNA microarray analysis. For analysis of gene expression, two independent preparations of total RNA obtained from two batches of serum-stimulated and resting MEFs ($G3BP^{+/+}$ and $G3BP^{-/-}$) by the Tri-Reagent procedure were used. Following isolation of total RNA, double-stranded cDNA was synthesized by reverse transcriptase (Life Technologies) using a T7-$(dT)_{24}$ primer (5′-GGCCAG TGAATTGTAATACGACTCACTATAGGGAGGCGG-$[dT]_{24}$-3′). Biotin-labeled antisense cRNA was transcribed from cDNA templates using T7 RNA polymerase (Enzo Biochem) and hybridized to oligonucleotide microarrays (U74A v2; Affymetrix), each containing 12,488 functional oligonucleotide probe sets. The probe array and the hybridization levels were measured with the HP GeneArray scanner after staining of the array with streptavidin-phycoerythrin. The GeneChip software analysis program MAS 4.1 and DMT 2.0 (Affymetrix) were used for the analysis of gene expression and expression clustering, respectively. Hybridization intensities (average differences) and assessments of the presence or absence of a given transcript (absolute call) were determined using the Affymetrix microarray suite. Average differences associated with transcripts judged to be present in the RNA pools were further analyzed using GeneSpring 4.0 (Silicon Genetics). The signal intensity of each probe was normalized to the median value of all intensities measured in the corresponding array. These array-normalized intensities were further normalized to the median of all array-normalized intensities determined for that gene over all hybridizations. Statistical comparisons of normalized wild-type and mutant intensities were performed using Welch's approximate *t* test with a significance cutoff at a *P* value of <0.01. Hierarchical clustering was performed using the Pearson correlation coefficient as a distance metric. The raw data have been successfully deposited in a MIAME-compliant format and can be accessed by logging into Array Express with username "tazi" and password "stiabr3e."

IP and quantitative RT-PCR. Immunoprecipitations (IPs) were performed with the anti-G3BP monoclonal antibody (1F1), anti-AUF1 (Upstate), or control anti-rabbit immunoglobulin G (IgG) as described previously (59). For quantitative RT-PCR analysis, total RNA was extracted from embryos and immunoprecipitates using Tri-Reagent (Sigma) according to the supplier's instructions. RQ1 DNase-treated RNA samples (5 μg) were reverse transcribed as described above. After first-strand synthesis, the cDNA was quantified by a ready-to-use reaction mixture for PCR containing Syber green I dye for real-time detection and quantification of the PCR product (QIAGEN). Fluorescence was detected with the LightCycler system (Roche Molecular Biochemicals). The primers used were as follows: IGF-II forward, GGCCCCGGAGAGACTCTGTGC, and reverse, GGAAGTCGTCCGGAAGTACGGC; GAS5 forward, CACCTCAAGT GAAGGCACTGC, and reverse, CACCTCAGAAACAAAGGTGCAG; β-tubulin forward, CGGACAGTGTGGCAACCAGATCGG, and reverse, TGGCC AAAAGGACCT GAGCGAACGG; and GAPDH forward, ACAGTCCATGC CATCACTGCC, and reverse, GCCTGCTTCACCACCTTCTTG. The amounts of IGF-II, GAS5, and β-tubulin mRNAs in each sample were quantified and normalized to the glyceraldehyde-3-phosphate dehydrogenase (*GAPDH*) content. Error bars resulted from three independent experiments (each measured in triplicate).

In vitro RNase assays. Radiolabeled *IGF-II* 3′ UTR and full-length *GAS5* RNAs were synthesized by in vitro transcription in the presence of 20 units of T3 or T7 RNA polymerase, respectively; 1 μg of the suitable linearized plasmids; and 5 μM [α-^{32}P]UTP (800 Ci/mmol) in 25-μl reaction mixtures according to the manufacturer's conditions. The RNase assays were performed as described previously (59).

RESULTS

Targeted disruption of the G3BP gene in mouse ES cells and generation of G3BP-deficient mice. The targeting strategy used to disrupt the G3BP sequence in mouse ES cells is illustrated in Fig. 1A. The targeting vector was constructed by replacing a 1.9-kb genomic fragment containing exons 2 and 3 of the *G3BP* gene with a promoterless β-*gal*–*neo* cassette. The β-*gal* sequences were inserted in frame with the authentic ATG start codon of *G3BP* in order to mimic the expression of G3BP in the deleted allele. In addition, a copy of the herpes simplex virus thymidine kinase gene was placed at the 3′ end of the construct. After electroporation and G418 selection, correctly targeted $G3BP^{+/-}$ ES cell lines were used to generate chimeric animals. Two independently targeted ES cell clones transmitted the mutation into the germ line. Mice homozygous for the targeted allele ($G3BP^{-/-}$) were generated by intercrosses of

A

Crosses type (Number of crosses)	Genotype (%)				Newborn death/ Total (%)			
	+/+	+/-	-/-	Total	+/+	+/-	-/-	Total
Female +/+ X Male +/- (30)	79 (56.8%)	60 (43.1%)		139	08/79 (10.1%)	13/60 (21.6%)		21/139 (15,8%)
Female +/- X Male +/+ (22)	54 (50.0%)	54 (50.0%)		108	28/54 (51.8%)	32/54 (59.2%)		60/108 (57.0%)
Female +/- X Male +/- (25)	40 (35.0%)	58 (50.8%)	16 (14.0%)	114	10/40 (25.0%)	23/58 (39.6%)	16/16 (100%)	49/114 (54.8%)

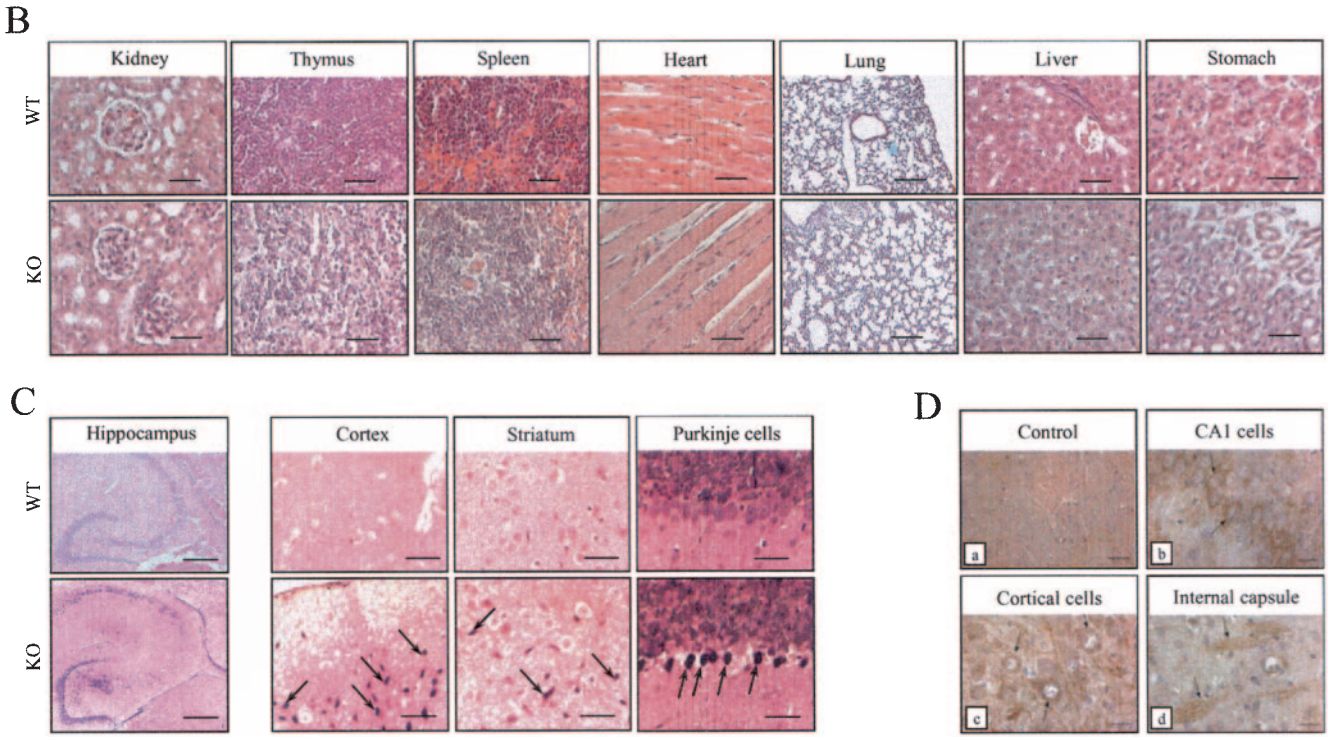

FIG. 2. Neonatal lethality of G3BP KO mice and histological evaluation. (A) Genotype distribution of progeny from heterozygous mating at birth. Statistical distribution of dead newborn mice stemming from either heterozygous mating or heterozygous/wild-type mating. (B) Histological analysis of $G3BP^{-/-}$ mouse organs after caesarean section at E18.5. Celestine/fuchsin staining of kidney, thymus, spleen, heart, lung, liver, and stomach showed no difference between wild-type and KO mice. Bars, 12.5 μm. (C) Staining of different regions of central nervous system: cortex, striatum, and cerebellum showed pyknotic cells, which appeared bright red on examination under the light microscope. Hippocampus bars, 5 μm. Cortex, striatum, and purkinje cell bars, 30 μm. (D) Immunostaining with antibodies that recognize the active form of caspase 3 in brain tissues from caesarean-section neonates of $G3BP^{-/-}$ mice. As indicated by arrows, extensive caspase 3 immunoreactivity appeared in the CA1 pyramidal cells of the hippocampus (b), in the cortex (c), and in some cells and fibers of the internal capsule (d). No caspase 3 immunoreactivity was observed in the wild-type cortex (a). Bars, 25 μm.

heterozygous ($G3BP^{+/-}$) mice, and the genotypes of the resulting embryos were determined by Southern blot analysis with a 3′-flanking probe (Fig. 1B, left). EcoRI digestion of wild-type and targeted G3BP loci gave rise to 9.5- and 4.5-kb bands, respectively. It is evident that homozygous mutant embryos (−/−) at E18.5 (days postcoitum) carried two targeted loci as expected. PCRs of genomic DNA with specific primers were consistent with Southern blotting (Fig. 1B, right) and were subsequently used for genotyping. Northern blot analysis of total RNA isolated from a G3BP embryo at E18.5 showed no significant hybridization to a mouse G3BP cDNA probe, whereas a wild-type $G3BP^{+/+}$ embryo contained G3BP mRNA, indicating the absence of any detectable transcript for the gene in the mutant animals (data not shown). Furthermore, RT-PCR of RNA derived from $G3BP^{-/-}$ embryos using primers spanning different parts of G3BP cDNA did not reveal any detectable amplification fragment, whereas fragments of the expected size were readily visible in littermate wild-type embryos (Fig. 1C). Western blot analysis revealed that $G3BP^{-/-}$ embryos at any embryonic stage (only E12.5 is shown) synthesized no detectable G3BP protein (Fig. 1D, left, lane 3), whereas $G3BP^{+/-}$ littermate embryos showed an expected 50% reduction compared to the wild type (Fig. 1D, left, compare lanes 1 and 2). As expected, probing the same blot with anti-β-Gal antibody confirmed the concomitant expression of β-Gal in $G3BP^{+/-}$ and $G3BP^{-/-}$ embryos (Fig. 1D,

right, lanes 2 and 3). Therefore, we conclude that *G3BP*$^{-/-}$ mutant embryos carry β-Gal instead of G3BP activity.

Disruption of G3BP results in neonatal lethality. Mice heterozygous for the *G3BP* disruption (*G3BP*$^{+/-}$) were indistinguishable from wild-type littermates at the adult stage. However, heterozygote intercrosses failed to produce viable mice homozygous for the mutation (*G3BP*$^{-/-}$) in >100 offspring (Fig. 2A). Moreover, *G3BP*$^{+/-}$ and *G3BP*$^{+/+}$ were found in normal Mendelian ratios of ~2:1, while offspring homozygous for the targeted mutation were detected at a frequency half of that predicted by Mendelian laws, indicating that *G3BP*$^{-/-}$ is lethal during fetal development. This pattern of partial embryonic lethality and neonatal death was observed with *G3BP*$^{-/-}$ mice generated from both ES cell lines used to raise gene-targeted mice and was not due to a peculiarity of the recombinant ES cell line. To examine whether G3BP$^{-/-}$ mice die before or after birth, we dissected embryos at E18.5 from the uteri of *G3BP*$^{+/-}$ intercrosses (caesarean section). Half of the resulting wild-type (n = 10) and *G3BP*$^{+/-}$ (n = 26) neonates were breathing and acquired a normal pink coloration. Conversely, all eight *G3BP*$^{-/-}$ neonates were pale, failed to breath, and showed cyanosis; these neonates could respond to pain stimulus when their tails were pinched with forceps, but they rapidly lost the reflex action within 15 min, demonstrating that the mutant mice were indeed alive for a very short period after the section. The other half of wild-type and *G3BP*$^{+/-}$ neonates were alive for a longer period (1 h), but they too died.

Crosses between heterozygous and wild-type mice revealed that the high frequency of death of neonates from *G3BP*$^{+/-}$ crosses has a maternal origin (Fig. 2A). While only 15% of newborn mice stemming from heterozygous males crossed with wild-type females died, a higher frequency of death (57%) was observed when heterozygous females were mated with wild-type males. In addition, implantation and development of fostered embryos from *G3BP*$^{+/-}$ crosses into wild-type mice completely abrogated the neonatal lethality of *G3BP*$^{+/-}$ and *G3BP*$^{+/+}$, implying that the expression level of G3BP in females determines survival at birth. However, we never succeeded in obtaining growing and/or viable *G3BP*$^{-/-}$ embryos after transplantation into wild-type mice, suggesting that *G3BP*$^{-/-}$ eggs are extremely vulnerable and consequently not able to resist damage from the manipulations.

We also tested the possibility that *G3BP* itself is subjected to genomic imprinting (17), since deletion of the maternal allele would affect the expression of G3BP much more than deletion of the paternal allele if it is expressed from the maternally inherited allele predominantly. We therefore determined the allele-specific expression status of G3BP in hybrid embryos obtained by crossing BALB/c females with JF1 (*Mus musculus molossinus*) males. Different embryonic and fetal stages were analyzed, as well as their placentas and yolk sacs. Maternal and paternal allele-specific RT-PCR products were distinguished by electrophoretic separation of single-strand conformation polymorphisms between BALB/c (maternal allele) and JF1 (paternal allele). At all stages analyzed, we detected comparable levels of G3BP expression from the maternal and the paternal alleles in the embryo proper and the extraembryonic membranes (data not shown). This established that G3BP is not imprinted during these embryonic and fetal stages. The strong phenotypic effects observed upon maternal transmission of the targeted deletion could therefore be due, at least in part, to a classical maternal effect (12) related to the presence of maternally produced protein in the egg.

Extensive neuronal-cell death in G3BP-deficient neonates. Anatomical and histological examination of the *G3BP*$^{-/-}$ neonates showed that all organs were present and of normal size, like those of wild-type or *G3BP*$^{+/-}$ littermates. The lungs of some, but not all, postnatal *G3BP*$^{-/-}$ pups showed a reduction in alveolar volume compared with those of living wild-type littermates (data not shown), whereas inflated lungs from *G3BP*$^{-/-}$ pups appeared histologically normal (Fig. 2B). To identify specific pathological abnormalities in *G3BP*$^{-/-}$ mice that might cause neonatal death, we performed other histological evaluations of hematoxylin- and eosin-stained sections (Fig. 2B). Among all tissues examined, the only marked abnormality was severe cell death in the nervous system in *G3BP*$^{-/-}$ pups compared with live wild-type neonates (Fig. 2C). In the mutant brain sections, we observed a significantly larger number of cells with pyknotic nuclei, which signifies the process of cell death in several regions of the central nervous system (Fig. 2C).

We next performed immunohistological staining with caspase 3-specific antibodies to detect apoptotic cells in wild-type and *G3BP*$^{-/-}$ embryo brains from two litters (Fig. 2D). This was performed by using an antibody that recognizes only the cleaved form of caspase 3, which is considered a specific marker of apoptotic cell death. A greatly increased number of caspase 3-positive cells was found in the CA1 pyramidal cells of the hippocampus, cortical cells, and internal capsule cells in *G3BP*$^{-/-}$ neonates (Fig. 2D) compared with wild-type controls. These caspase-positive cells were observed to be pyknotic. Neither caspase-positive nor pyknotic cells were detected in other organs, such as the lungs, muscle, heart, intestine, and liver (Fig. 2B). These data indicate that a severe induction of apoptotic cell death in the central nervous system of G3BP$^{-/-}$ neonates is the major histological defect. In histological sections, there were no apparent cardiovascular abnormalities or defects in kidneys, thymus, spleen, heart, lung, liver, muscle, or stomach, although in several *G3BP*$^{-/-}$ neonates, hemorrhaging was also evident in the brain, indicating that neuronal-cell death was not a result of brain irrigation. Therefore, it appears likely that lethality in *G3BP*$^{-/-}$ mice results from massive neuronal-cell death in the central nervous system.

Fetal growth retardation of G3BP-deficient embryos. To rigorously determine whether *G3BP* deficiency results in a partial embryonic-lethal phenotype and to establish the point in gestation at which *G3BP*$^{-/-}$ mice suffer developmental arrest, embryos were phenotypically (Fig. 3C) and genetically (Fig. 3A) evaluated at various time points during gestation by PCR of yolk sac tissue. The results of genotyping summarized in Fig. 3A did not reveal gross loss of *G3BP*$^{-/-}$ embryos at any particular developmental stage. All embryos were recovered at the frequencies predicted by Mendelian law. However, reproducibly, some *G3BP*$^{-/-}$ embryos were reduced in size in comparison with littermates at all embryonic stages analyzed. This was confirmed by quantitative analysis of the weights of the embryos at different stages of development (Fig. 3B). The retardation in growth and development was increasingly apparent at later stages, where *G3BP*$^{-/-}$ embryos displayed dor-

A

Day (Number of litters)	Number of embryos +/+	+/-	-/-	Total
E11.5 (7 litters)	14 (25.0%)	30 (53.5%)	12 (21.4%)	56
E12.5 (9 litters)	15 (26.7%)	29 (51.7%)	12 (21.4%)	56
E13.5 (7 litters)	08 (23.5%)	17 (50.0%)	09 (26.0%)	34
E15.5 (6 litters)	10 (30.0%)	15 (45.4%)	08 (24.2%)	33
E17.5 (5 litters)	08 (22.2%)	20 (55.5%)	08 (22.2%)	36
P0 (25 litters)	40 (35.0%)	58 (50.8%)	16 (14.0%)	114

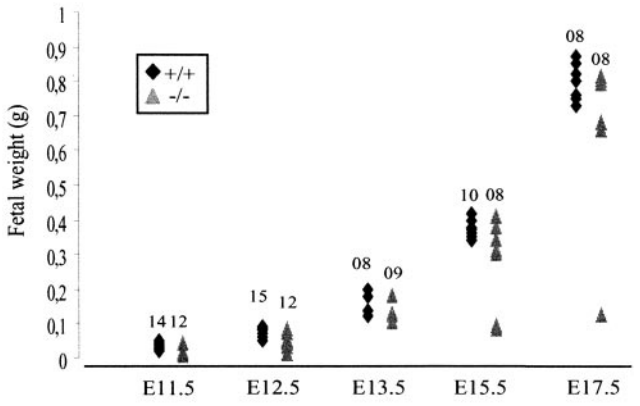

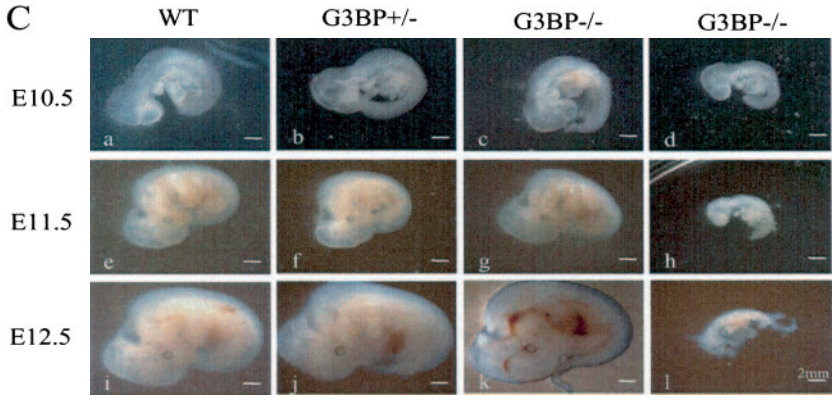

FIG. 3. Growth abnormalities in G3BP KO mice. (A) Genotype distribution of progeny from heterozygous mating at various developmental stages. (B) Fetal weight of G3BP mutants (−/−) and wild-type littermates (+/+) at the indicated gestational stages. Each symbol represents a single embryo (superimposed in some cases), with the total number of weighed embryos indicated at the top. The data are from the same litters as in panel A. The average weights (in g) ± standard error were as follows: E11.5, $G3BP^{+/+} = 0.036 \pm 0.009$, $G3BP^{-/-} = 0.019 \pm 0.017$, $P < 0.001$; E12.5, $G3BP^{+/+} = 0.078 \pm 0.012$, $G3BP^{-/-} = 0.049 \pm 0.025$, $P < 0.001$; E13.5, $G3BP^{+/+} = 0.172 \pm 0.030$, $G3BP^{-/-} = 0.108 \pm 0.042$, $P < 0.001$; E15.5, $G3BP^{+/+} = 0.375 \pm 0.026$, $G3BP^{-/-} = 0.281 \pm 0.126$, $P < 0.001$; E17.5, $G3BP^{+/+} = 0.790 \pm 0.049$, $G3BP^{-/-} = 0.640 \pm 0.295$, $P < 0.001$. (C) Comparison of the sizes of the wild type and heterozygous ($G3BP^{+/-}$) and G3BP null ($G3BP^{-/-}$) mutants at different embryonic stages.

sal truncation and stunted tails and cranial defects (Fig. 3C, d, h, and l). No such abnormalities were evident in wild-type (Fig. 3C, a, e, and i), $G3BP^{+/-}$ (Fig. 3C, b, f, and j), or $G3BP^{-/-}$ (Fig. 3C, c, g, and k) littermates that had normal growth. It is therefore possible that G3BP controls the expression of genes involved in the growth of embryos (see below). The widespread expression of G3BP in embryos is consistent with this possibility (data not shown).

Impaired proliferation of G3BP$^{-/-}$ MEFs in vitro and transcriptome analysis. The complex biological properties associated with G3BP deficiency prompted us to carry out transcriptional profiling of wild-type and $G3BP^{-/-}$ cells to identify potential mRNA targets of G3BP. The widespread expression of G3BP in the various mouse tissues, together with our previous finding that G3BP associates with specific mRNA targets in primary MEFs, prompted us to establish the cellular consequences of G3BP loss in MEFs. We first examined whether the absence of G3BP influences the proliferation rate of MEFs isolated from different E14.5 $G3BP^{-/-}$ embryos ($n = 6$). Western blotting confirmed that the $G3BP^{-/-}$ MEFs no longer expressed the G3BP protein. As shown in Fig. 4A, early-passage $G3BP^{-/-}$ MEFs (less than passage 5) show a significantly reduced proliferation rate compared with controls, and after 8 days in culture, their cumulative cell numbers reached only 35% of the value obtained with the controls. However, except for this reduced proliferation capacity, morphologically the cultured $G3BP^{-/-}$ cells were indistinguishable from wild-type $G3BP^{+/+}$ cells. The cell cycle distribution of asynchronously growing MEFs was also unaffected by G3BP loss (Fig. 4B), excluding the possibility that G3BP is involved in cell cycle control. Since G3BP was identified as associated with Ras GTPase-activating protein (57), we also tested whether the absence of G3BP affects signaling pathways mediated by Ras. Quiescent $G3BP^{-/-}$ and $G3BP^{+/+}$ MEFs were stimulated for 15 min or 30 min with serum, and specific phosphorylation of ERK and AKT signaling proteins activated downstream of Ras was revealed by phosphospecific antibodies. Figure 4C shows that G3BP depletion did not affect either factor's phosphorylation, implying that G3BP is unlikely to play a major role in transduction of signals upstream of ERK1/2 and AKT. However, given that addition of growth factors did not stimulate $G3BP^{-/-}$ MEFs to divide, it is likely that G3BP deficiency is accompanied by cellular lesions that may lead to senescence and/or longer doubling time than for wild-type MEFs.

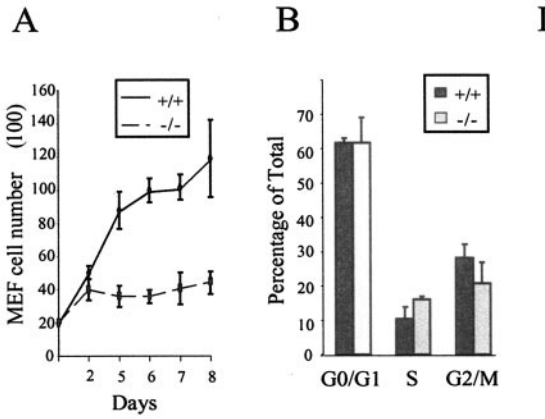

D

Families and genes	GenBank no.	Fold change in Proliferating cells	Fold change in Resting cells
Proliferation, differentiation and signalling			
LIM and SH3 protein 1	U58882	>-10	>-10
Cortactin	U03184	-6	-4
Four and a half LIM domains 1	NM_010211	-2.5	-1.2
Carboxyl terminal LIM domain protein (Ldb3)	AF053367	-2	-2
Fibroblast inducible secreted protein	M70642	-4	-1.2
* Growth factor receptor bound protein 10	U18996	>-4	-1
Thrombin receptor	L03529	-3.5	-1.5
Secretory protein SEC23	D12713	-3.5	-1
Placentaspecifc 8	NM_139198	-3	-3
Rab 7, pseudogene 1	Y13361	-3	-3
Plasminogen activator inhibitor (PAI)	M33960	-3	-1
Adipose differentiation related protein	M93275	-2.8	-2
Mouse Cyr61	M32490	-2.7	-1.2
Small inducible cytokine A7	X70058	-2.5	-1.1
Connective tissue growth factor related protein WISP	AF100778	-2.5	-1
Lectin lambda	U56734	-2	-1.8
Solute carrier family 2	M22998	-2	-1.5
Small inducible cytokine A2	M19681	-2	-1.2
* H19 fetal liver mRNA	X58196	+1.8	+1.6
Retinoic acide-binding protein	M35523	+1.8	+2.1
Integral membrane protein 2	L38971	+2	+2
Osteoglycin	D31951	+2	+2
Retinoic acid binding protein	X15789	+2	+2
§ Growth arrest specific 1	X65128	+2.1	+2.2
Clusterin	D14077	+2.3	+2.3
Chemokine orphan receptor 1	AF000236	+2.4	+2
* Cyclindependent kinase inhibitor 1C	U22399	+2.47	+2.3
Connexin 43	M63801	+2.5	+2.5
§ Growth arrest specific 2	M21828	+2.7	+2.25
G protein signaling regulator RGS2	U67187	+2.8	nd
Tetra;voltage gated potassium channel activity	NM177715	+2.8	+2.4
Interleukin 1 receptor antagonist	L32838	+3	+2,59
Calmodulin-like 4	NM138304	+3	+2.8
* Insulin Like growth factor 2	X71922	+4	+4
Secreted frizzled related protein sFRP	U88567	+5.5	+5.5
* Delta-like 1 homolog	Z12171	+5.6	+4
§ Growth arrest specific 5	NM_013525	+14.8	+17
DNA binding proteins and transcription			
Nuclear factor erythroid related factor 1 (Nrf1)	AF015881	>-3	>-3
Sine oculis related homeobox 1	X80339	+2	nd
Proline rich nuclear receptor coactivator 2	NM026383	+2	+1
Histone H2A.FIZ	C5300021.11	+2	+1.5
Structural maintenance of chromosomes 4	NM133786	+2	+2
Inhibitor of DNA binding 2	AF077861	+3	+2
NfiB1-protein	Y07685	+3	+2
Structural proteins			
Actin, alpha 1	M12347	-2	-2
Junction plakoglobin	M90365	-2	-1.5
RNA, U22 small nucleolar	AK036616	+1.8	+1.8
Lumican	MF013262	+4	+4
Miscellaneous genes			
Cardiac ankyrin repeat protein MCARP	AF041847	-3	-2
Cysteine rich protein	D88793	-2	-2
Protein disulfide isomerase related protein	AW045202	-2	-2
Mouse pentylenetetrazol related mRNA	D45203	+1.8	+2
mRNA for mKIAA1635 protein	AI644072	+2	+1.8

FIG. 4. Proliferation, signaling, and G3BP target gene expression in G3BP mutant MEFs. (A) Wild-type and *G3BP*$^{-/-}$ MEFs (passage 3) plated at low density (2×10^3 cells/6-cm dish) and cultured for 8 days. Each value is the average of three independent experiments with duplicate plates. The error bars indicate standard deviations. (B) Cell cycle distribution of asynchronously growing G3BP mutant MEFs. (C) Activation of Akt and Erk1/2 pathways in the absence of G3BP. Wild-type (lanes 1 to 3) and *G3BP*$^{-/-}$ (lanes 4 to 6) MEFs were starved for 24 h by serum deprivation (lanes 1 and 4) and stimulated for 15 (lanes 2 and 5) or 30 (lanes 3 and 6) min with serum. Proteins were immunoblotted with anti-phospho-Erk, anti-phospho-Akt, or anti-Akt antibody. (D) Summary of differentially expressed transcripts from wild-type and G3BP mutant MEFs, identified by Affymetrix microarray. The changes were calculated from analyses performed with cRNA probes from serum-stimulated cells and serum-starved cells. The negative and positive changes correspond to down- and up-regulated genes in G3BP mutant MEFs, respectively. Imprinted genes are marked by *, and growth arrest-specific genes by §.

To determine whether the absence of G3BP alters the expression of genes involved in cellular proliferation and/or growth arrest, we performed a differential analysis of RNA transcripts isolated from quiescent or dividing wild-type and *G3BP*$^{-/-}$ MEFs. Biotinylated cRNAs synthesized from purified RNA were hybridized to the Affymetrix Mouse Gene Chip Mu74 containing over 12,000 oligonucleotide probe sets. To minimize differences resulting from intergroup variation, cRNA probes were prepared from pooled clones of *G3BP*$^{+/+}$ or *G3BP*$^{-/-}$ MEFs, each obtained from different embryos. The experiment, as initiated from growth and serum starvation, was performed independently two times using cRNA probes from independently prepared MEF pools. Hybridization signals generated from wild-type and *G3BP*$^{-/-}$ RNA sets were compared. After elimination of data points that were suspected because of low signal or high background, a total of 53 genes exhibiting differential expression ($P < 0.05$) were grouped by functional clustering (Fig. 4D). Notably, the number of genes whose transcript levels underwent at least a threefold increase relative to those from wild-type cells in the two experiments is very close to that of down-regulated genes (Fig. 4D), indicating that lack of G3BP does not affect transcriptional processes in a uniform way. Interestingly, however, 70% of differentially expressed genes are implicated in cell signaling and control of cellular proliferation, demonstrating that these factors may relay, propagate, and amplify the biological functions of G3BP through subsequent transcriptional control.

Of the 12,000 genes, only 5 genes were induced fourfold or more in the absence of G3BP (Growth arrest specific 5 [*GAS5*], Secreted frizzled-related protein 2 [*SFRP2*], Delta-like homolog 1 [*Dlk1*], Insulin-like growth factor II [*IGF-II*], and *Lumican*). These genes contain putative G3BP binding sites, previously established by SELEX (59), situated at one position (75 to 85) of *Gas5* mRNA, one position (2765 to 2777) of *IGF-II* mRNA, two positions (478 to 509 and 603 to 614) of *SFRP* mRNA, three positions (233 to 244, 925 to 936, and 1323 to 1334) of *Dlk1* mRNA, and one position (227 to 238) of *Lumican* mRNA (nucleotide positions are according to Gen-

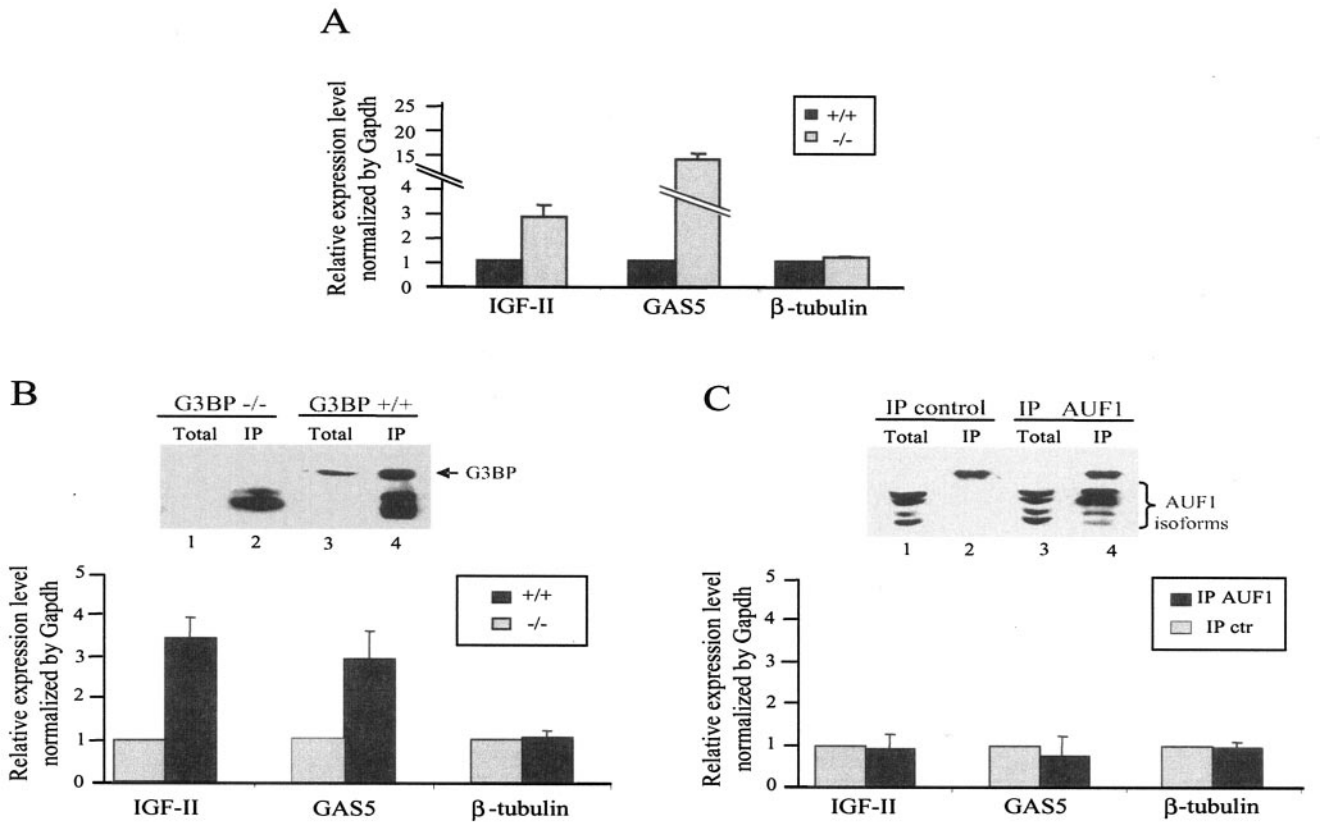

FIG. 5. Identification of *IGF-II* and *GAS5* mRNAs as specific targets of G3BP. (A) Quantitative RT-PCR was used to rigorously quantify the changes in *IGF-II* and *GAS5* mRNA levels observed by microarray analysis. The values are the averages of three independent experiments, and the level of expression is normalized with that of the internal control gene (*GAPDH*). The error bars indicate standard deviations. No change was observed for the β-*tubulin* gene (control). (B) G3BP was affinity purified with an anti-G3BP antibody (1F1) immobilized on protein G-Sepharose from total extracts of proliferating $G3BP^{+/+}$ and $G3BP^{-/-}$ MEFs (for *IGF-II* and β-*tubulin* mRNA analyses) or resting MEFs (for *GAS5* mRNA analysis). (C) mRNP complexes were affinity purified with either anti-AUF1 or anti-rabbit IgG antibodies immobilized on protein A-Sepharose. Immunoprecipitates and corresponding supernatants were analyzed by immunoblotting using anti-G3BP or anti-AUF1 antibodies (top). RNAs associated with affinity-purified G3BP, AUF1, or IgG (IP control) were analyzed by quantitative RT-PCR (bottom). The values are the averages of three independent experiments, and the level of expression is normalized with that of the internal control gene (*GAPDH* mRNA).

Bank reference numbers in Fig. 4D). Therefore, *Gas*, *SFRP*, *Dlk*, and *Lumican* mRNAs constitute potential targets of the RNA-cleaving activity of G3BP. Because deregulation of the expression of the *IGF-II* and *GAS5* genes is expected to disturb fetal growth and/or cell proliferation, these genes were chosen for subsequent analysis. IGF-II is an important regulator of growth and differentiation of many tissues (15, 16), and *GAS5* is a non-protein-coding multiple small nucleolar RNA (snoRNA) host gene that was initially discovered in a screen for potential tumor suppressor genes expressed at high levels during growth arrest (13, 50). More importantly, both *IGF-II* and *GAS5* genes have been shown to be regulated posttranscriptionally, and a specific endonucleolytic cleavage was shown to regulate *IGF-II* mRNA stability (13, 37). Thus, G3BP appears to be a likely candidate to trigger *IGF-II* and *GAS5* mRNA degradation.

G3BP controls the expression levels of *GAS5* and *IGF-II* mRNAs in MEFs. To further evaluate the effect of G3BP depletion on *IGF-II* and *Gas5* expression, we used real-time RT-PCR to analyze the changes in mRNA levels. cDNA was produced using total RNA as a substrate. The relative amount of each sample was determined with a standard curve obtained by amplifying a 10-fold dilution series of cDNA that was prepared by PCR. The highest value was set as 100%, and the values of the other samples were calculated relative to this value. In agreement with microarray data, the results indicated that in $G3BP^{-/-}$ cells the induction of *IGF-II* mRNA compared with wild-type cells was 3.5- ± 1.6-fold ($P < 0.001$) using *GAPDH* mRNA as a reference. A significantly higher *GAS5* (15 ± 1.6) mRNA content was found in $G3BP^{-/-}$ cells than in wild-type cells (Fig. 5A). No significant difference was found in *GAPDH* mRNA levels among all RT samples (data not shown), implying that the relative amounts of RNA were consistent among those samples. Furthermore, no change in the expression level of β-*tubulin* mRNA was observed between $G3BP^{-/-}$ and wild-type cells (Fig. 5A), indicating that the absence of G3BP allows selective accumulation of *IGF-II* and *GAS5* mRNAs.

If *IGF-II* and *GAS5* mRNAs are specific targets for G3BP's cleaving activity, they are expected to associate with G3BP. To test this hypothesis more directly, RNAs interacting with G3BP were recovered by immunoprecipitation from total ex-

tracts prepared from quiescent or dividing wild-type MEFs by using G3BP-specific antibodies. Western blot analysis established that G3BP was efficiently depleted from wild-type MEF extracts following immunoprecipitation (Fig. 5B, top, lane 4). As a negative control, the same immunoprecipitation experiments were performed using *G3BP*$^{-/-}$ MEFs (Fig. 5B, lane 2). RNAs recovered in these complexes were analyzed by real-time RT-PCR using the oligo(dT) for priming the first-strand DNA synthesis and specific primers for *IGF-II*, *GAS5*, or *GAPDH* mRNA. In order to determine the association efficiency of each mRNA transcript with G3BP, the background amount associated with the antibodies in the control immunoprecipitations normalized to GAPDH was set as 1. The results in Fig. 5B (bottom) clearly show that *IGF-II* and *GAS5*, but not β-*tubulin*, were among mRNAs efficiently selected by G3BP from wild-type MEFs. However, all these mRNAs were also detected from the supernatants of immunoprecipitations (data not shown), indicating that only a fraction of *IGF-II* and *GAS5* mRNAs were associated with G3BP and thus could be affected by G3BP-mediated degradation. Alternatively, the stringent conditions used for the immunoprecipitation (1% Triton) could also account for some loss of mRNAs associated with G3BP. In agreement with the idea that G3BP is involved in the control of the fate of mRNAs, it is also notable that G3BP antibodies fail to immunoprecipitate *GAS5* mRNA from dividing cells that contain very low levels of this mRNA (data not shown). The possibility that G3BP reassociates with this endogenous mRNA following extraction can be ruled out, because immunoprecipitation from *G3BP*$^{-/-}$ extracts complemented with recombinant G3BP failed to reveal any specific association with target mRNAs (data not shown).

To further confirm the specificity of association of G3BP with *GAS5* and *IGF-II* mRNAs, we tested the abilities of these mRNAs to be immunoprecipitated by an antibody directed against AUF1, an RNA binding protein containing an RRM domain and shown to regulate the stability of mRNAs with AU-rich elements (64). AUF1 is expressed in four isoforms (p37, p40, p42, and p45) that were readily detected in G3BP$^{+/+}$ MEFs by a polyclonal antibody (Fig. 5C, top, lanes 1 and 3). While AUF1 isoforms were efficiently immunoprecipitated by the antibody (Fig. 5C, top, lane 4), neither *GAS5* nor *IGF-II* cDNA was effectively amplified from AUF1 IPs, implying that they are uniquely associated with G3BP but not AUF1 (Fig. 5C, bottom). Consistent with this view, Western blot analysis of the same IPs did not reveal any association between AUF1 and G3BP (data not shown).

Since *IGF-II* and *GAS5* mRNAs contained a single putative binding site for G3BP, we assessed both their cleavage in vitro by recombinant G3BP and their decay rates in G3BP$^{-/-}$ MEFs compared to G3BP$^{+/+}$ MEFs. As expected, in vitro-transcribed ^{32}P-labeled *IGF-II* and *GAS5* RNAs were efficiently and completely cleaved after 6 min of incubation with 0.1 U of recombinant G3BP (Fig. 6A) following the same kinetics of cleavage as the 3′ UTR of c-*myc* mRNA, which contained a single G3BP binding site (59).

To determine if the absence of G3BP alters the stability of *IGF-II* and *GAS5* mRNAs, quiescent G3BP$^{+/+}$ or G3BP$^{-/-}$ MEFs were stimulated with serum for 1 h and then exposed to actinomycin D to inhibit transcription. RNAs were isolated at various times after inhibition of transcription, and the levels of *IGF-II* and *GAS5* mRNAs were measured and normalized to *GAPDH* mRNA levels using RT followed by real-time PCR analysis. Each time point was repeated three times, and the quantified data are presented graphically in Fig. 6B. This analysis demonstrated that *IGF-II* and *GAS5* decayed more rapidly in wild-type MEFs than in *G3BP*$^{-/-}$ MEFs, whereas decay of β-*tubulin* mRNA was unaffected (Fig. 6B). In *G3BP*$^{-/-}$ MEFs, the half-lives of *IGF-II* and *GAS5* mRNAs were longer than 4 h, while in wild-type MEFs, the half-lives were ~2 h for *IGF-II* mRNA and ~1 h for *GAS5* mRNA. Altogether, these findings are in complete agreement with steady-state mRNA measurements and are consistent with the hypothesis that G3BP modulates the degradation rates of its associated mRNAs. Thus, G3BP is part of mRNPs controlling the fate of *IGF-II* and *GAS5* mRNAs.

Dynamic control of *GAS5* and *IGF-II* mRNA expression by G3BP during mouse development. To determine whether G3BP deficiency leads to alteration of the expression of *IGF-II* and *GAS5* mRNAs during mouse development, total RNA was extracted from embryos at various time points during gestation and then assayed for *IGF-II* and *GAS5* mRNA expression by real-time RT-PCR. Three embryos of the same size from each embryonic stage were used to quantitate the level of each mRNA. To compare the expression level of each mRNA between different embryonic developmental stages, the expression in the wild-type strains normalized to GAPDH was set as 1. Unexpectedly, low levels of *IGF-II* and *GAS5* mRNAs were observed at E12.5 in *G3BP*$^{-/-}$ mice compared to the wild type (Fig. 7A), whereas no changes in the expression of tubulin were observed at any developmental stage. In contrast, *IGF-II* and *GAS5* mRNAs were more abundant in *G3BP*$^{-/-}$ embryos at E13.5 of development and demonstrated a higher level of expression by day 15.5. It is noteworthy, however, that *GAS5* has a peak of expression by days 15 to 16 in the wild-type mice (13), which is likely to obscure a greater difference that may exist between wild-type and *G3BP*$^{-/-}$ mice. At birth, the expression level of *IGF-II* was comparable to that of the wild type, whereas the *GAS5* mRNA expression level was still very high. These results suggest that G3BP is required for correct expression of these genes at different stages of development.

Altered expression of *IGF-II* has been shown to influence fetal growth (15), and it was important to determine whether the absence of G3BP affects the spatial and temporal distribution of this mRNA at different stages of development. Given that major changes occurred between E12.5 and E15.5, we monitored the *IGF-II* gene expression by in situ hybridization of mice at these two embryonic stages. In agreement with RT-PCR data, less *IGF-II* mRNA was detected in *G3BP*$^{-/-}$ mouse embryos than in the wild type at E12.5 (Fig. 7B, compare a to c with d to f), whereas a higher level was observed at E15.5 (Fig. 7B, compare a and b with d to f). However, the expression patterns of *IGF-II* were identical in the wild-type and mutant mice, implying that G3BP did not alter *IGF-II* expression in a tissue-specific manner.

DISCUSSION

Consistent with the proposed role of G3BP in controlling the fate of mRNA in response to extracellular stimuli, these studies demonstrate that a total lack of G3BP in mice invari-

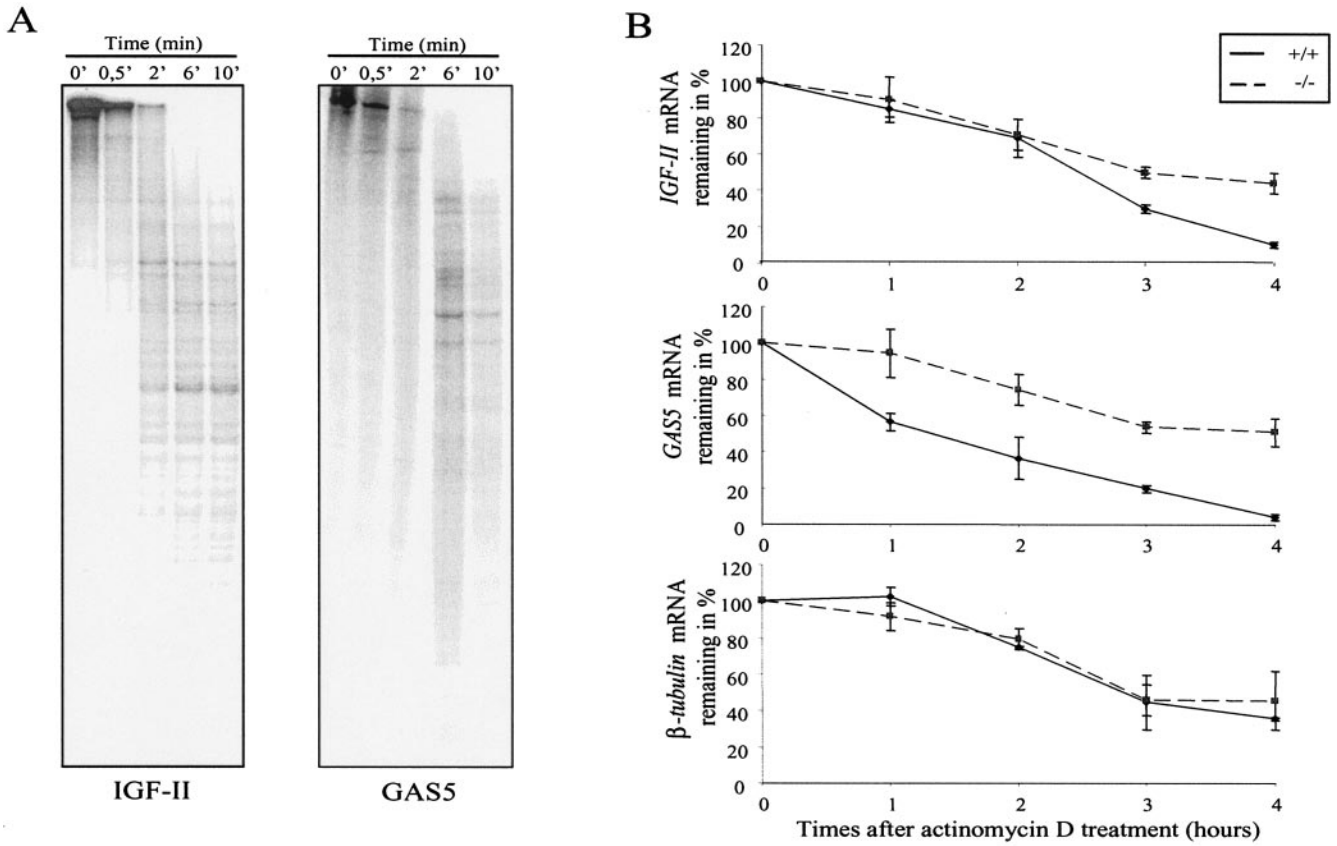

FIG. 6. (A) In vitro cleavage of *IGF-II* and *GAS5* mRNAs by purified recombinant G3BP. ^{32}P-labeled *IGF-II* 3′ UTR and *GAS5* RNA transcripts were incubated for the indicated times as described previously (59). RNase products were resolved on 5% polyacrylamide-8 M urea gels and revealed by autoradiography. (B) Comparison of *IGF-II*, *GAS5*, and β-*tubulin* mRNA decay in *G3BP*$^{+/+}$ and *G3BP*$^{-/-}$ MEFs. Quiescent cells were stimulated with serum for 1 h and treated with 5 μg of actinomycin D/ml. Total RNAs were extracted at the indicated times, and *IGF-II*, *GAS5*, and β-*tubulin* mRNAs were quantitated by real-time RT-PCR. All values were scaled to the level obtained from GAPDH quantifications. Error bars resulting from three independent experiments, each measured in duplicate, are shown. The error bars indicate standard deviations.

ably leads to fetal growth retardation and fatal neuronal-cell death events early in life. A comparison of the global gene expression profiles between wild-type and *G3BP*$^{-/-}$ MEFs correlated the phenotypes with altered expression of imprinted and growth arrest-specific genes, respectively. Our studies have also shown that developmental failures are frequent in *G3BP*$^{-/-}$ embryos, although embryonic G3BP is not strictly required for development to term. At least half of *G3BP*$^{-/-}$ embryos succeed in traversing the vulnerable period in development that seems to occur before E12.5. Because *G3BP*$^{-/-}$ mice can presently be raised only by breeding *G3BP*$^{+/-}$ mothers, maternally derived G3BP cannot be formally excluded as contributing to the (partial) developmental success of some *G3BP*$^{-/-}$ embryos. However, if early embryos do acquire any maternal G3BP, it is clear that the presence of a maternal reservoir is insufficient to maintain the development of all *G3BP*$^{-/-}$ embryos. The majority of *G3BP*$^{-/-}$ embryos that survived this period remained viable until birth.

A reduced level of G3BP in *G3BP*$^{+/-}$ mothers also leads to a high frequency of neonatal lethality in pups (Fig. 2). Whether this phenotype is independent or is an aspect of the phenotype associated with complete loss of G3BP is unknown. It can be envisioned that heterozygous males escaped this abnormal phenotype, probably as a result of their noninvolvement in complex nurturing behaviors. Alternatively, *G3BP* may represent another example of an imprinted gene inheritance, as postulated by Hall (22). Our data completely ruled out the possibility that *G3BP* is itself an imprinted gene (data not shown), and rather, show the involvement of G3BP in controlling the expression of imprinted genes (Fig. 4). As G3BP acts as a posttranscriptional regulator, the phenotype may arise primarily from the inappropriate expression of these genes in G3BP$^{+/-}$ females and/or their progeny. The misexpression of several imprinted genes (*IGF-II*, *Dlk1*, *H19*, *Gtl2*, *Growth factor receptor-bound protein 10*, and *cyclin-dependent kinase inhibitor 1C*) in G3BP$^{-/-}$ MEFs and during embryogenesis of KO mice is consistent with this hypothesis. These observations further support the idea that a parental-origin-specific gene regulation mechanism(s) involves not only well-established epigenetic modifications, like postsynthetic modification of DNA itself (i.e., DNA methylation) or of proteins associated with DNA (methyl-binding proteins and histones) (26, 33), but also posttranscriptional control, allowing remodeling of specific mRNPs (mRNA associated with proteins). G3BP knockout mice, therefore, constitute an interesting model system to determine how transcriptional and posttranscriptional controls

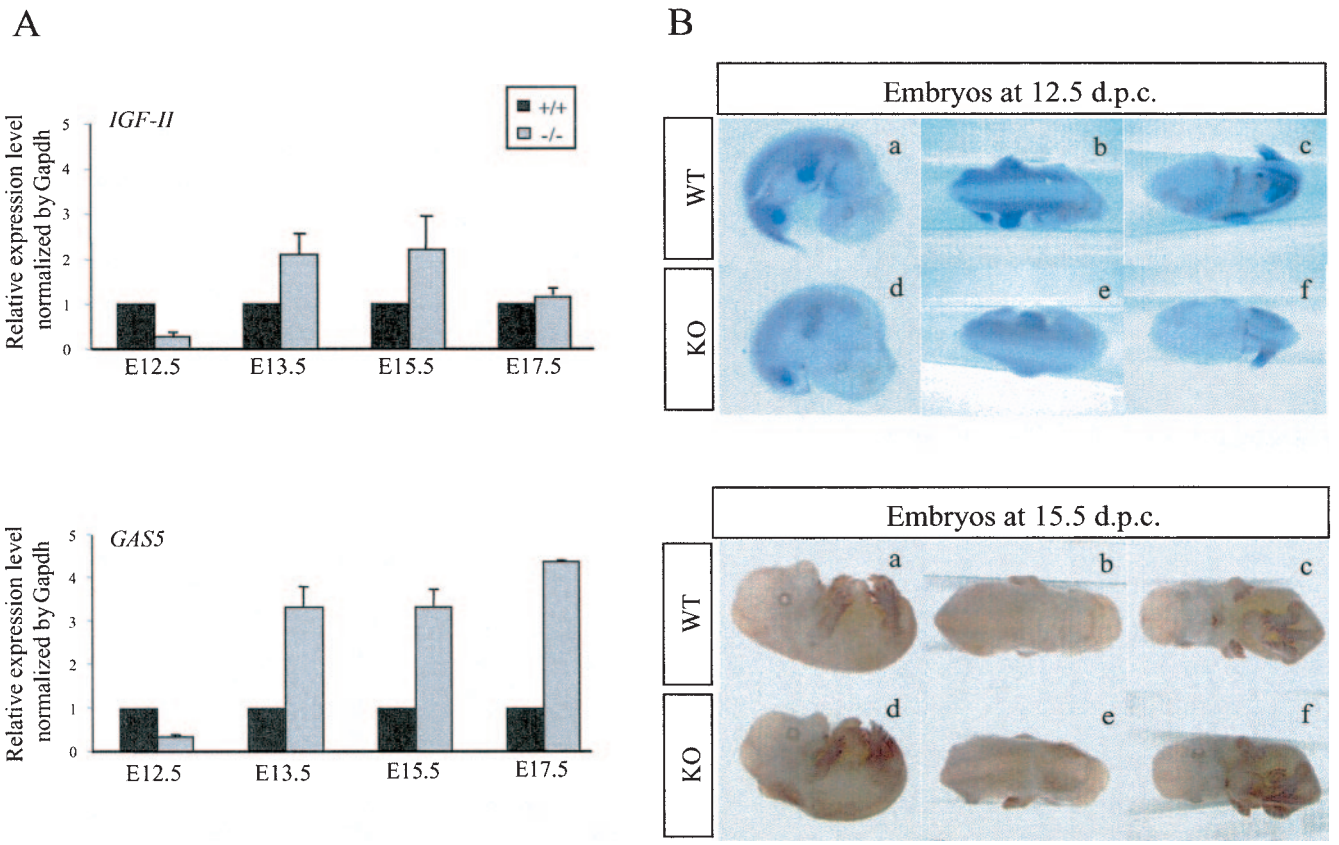

FIG. 7. Relative expression of *IGF-II* and *GAS5* mRNAs in G3BP null mutants at different embryonic stages. Total RNAs were prepared from embryos at the indicated stages of embryonic development. Relative expression of *IGF-II* and *GAS5* mRNAs in $G3BP^{-/-}$ embryos was analyzed by quantitative RT-PCR using specific primers. The expression in the wild-type strains normalized to *GAPDH* was set at 1 and compared to that in $G3BP^{-/-}$ embryos. Error bars resulting from three independent experiments (each measured in triplicate) are shown. The error bars indicate standard deviations. (B) *IGF-II* mRNA expression revealed by whole-mount in situ hybridization with an IGF-II antisense riboprobe was examined at E12.5 and E15.5 developmental stages. d.p.c., days postcoitum.

are orchestrated to contribute to a tight regulation of the expression of imprinted genes during development.

G3BP is expressed ubiquitously in both humans and mice, so the finding that disruption of the gene has a prominent and disproportionate effect on neuronal-cell death at birth is somewhat surprising. It may suggest that functional redundancy of G3BP function in the brain is less than in other tissues. Alternatively, brain homeostasis and development may be exquisitely dependent upon posttranscriptional gene regulation. It is known that neuronal differentiation involves the elaboration of morphologically distinct axons and dendrites, which are at a considerable distance from the nucleus and contain a small fraction of mRNAs (30, 45). Regulated expression of these differentially distributed mRNAs requires mechanisms for sorting, targeting, transport, and local translation/degradation processes (8, 34, 52). G3BP can take part of assembled mRNPs involved in the control of these processes and mediates both transport and translation/degradation of specific mRNA targets. In support of this hypothesis, G3BP was recently found to copurify with RNP particles containing tau mRNA and two other RNA binding proteins, namely, HuD and IGF-II mRNA binding protein 1 (IMP-1) from both neuronal-cell and mouse brain extracts (2). While the exact function(s) of these assembled particles is not known, it is thought that they might contribute to tau specialized localization and/or translation/degradation in developing neurones (1, 7, 53). Indeed, tau mRNA is among a growing family of mRNAs that are present as motile RNA-protein granules in dendrites and developing axons, where they are locally translated in response to external stimuli, growth factors, and translation inhibitors (1, 7, 53). It can be speculated that G3BP loss impedes this type of regulation and consequently leads to massive neuronal-cell death. The ability of G3BP to assemble cytoplasmic stress granules under stress conditions and the fact that this assembly process is regulated by Ras (58) and apoptosis-inducing factor (11) bring further support to this hypothesis.

Regulation of mRNA stability by G3BP can also help to explain the phenotypes associated with G3BP loss. Among mRNAs that are highly expressed in the absence of G3BP, *GAS5* mRNA constitutes an ideal target for the endoribonuclease activity of G3BP. *GAS5* is a non-protein-coding mRNA derived from a multi-small-nucleolar-RNA host gene that is a member of the 5′-terminal oligopyrimidine gene family (23, 50). Interestingly, increased levels of *GAS5* mRNA have been shown to result from posttranscriptional regulation in growth-arrested cells (13). Several lines of evidence support the notion that G3BP could play a role in this posttranscriptional control: (i) *GAS5* mRNA is tightly associated with G3BP

in arrested cells (Fig. 5B) and is degraded in vitro by purified G3BP (Fig. 6A); (ii) *GAS5* is more rapidly degraded in wild-type cells than in G3BP-deficient cells (Fig. 6B); and (iii) during growth arrest, *GAS5* mRNA, like G3BP, has been shown to cosediment in a sucrose gradient with mRNP particles (50). Moreover, G3BP and *GAS5* have the same spatial and temporal distributions during mouse development and are expressed in the brain (13). In addition, stable overexpression of *GAS5* mRNA in multipotent MK31 cells enhanced initial and terminal stages of neuronal differentiation and induced decreased cellular viability (46). This observation, together with other reports (19, 20, 27), is consistent with the idea that high levels of *GAS5* mRNA are directly involved in neuronal-cell death, and *GAS5* constitutes a potential candidate gene implicated in massive neuronal-cell death in the brains of G3BP knockout mice. A major goal for future studies will be to determine the function(s) of this non-protein-coding gene, besides hosting snoRNAs.

Deletion of G3BP also leads to dynamic changes in embryonic *IGF-II* mRNA expression during embryogenesis. *IGF-II* is one of several imprinted genes known to be important for proper fetal growth and development (3, 15, 16, 54), and its widespread expression is subject to complex posttranscriptional regulation (38). The coordinate expression of the three fetal *IGF-II* transcripts increases rapidly from ~E9.5 before reaching a maximal level around E12.5. Expression continues until a few days after birth, after which *IGF-II* transcripts become down-regulated. Both nuclear processing and export, as well as translational discrimination and regulation of mRNA stability, are believed to fine tune *IGF-II* expression during the embryonic period. *IGF-II* transcripts have previously been shown to be inactivated by endonucleolytic cleavage at G2183 in their common 3′ UTR (35, 37). Cleavage results in the release of a stable 1.8-kb fragment, but so far, we have no direct evidence that G3BP is involved in the process (data not shown). G3BP has a preference for CA residues, and although mutation of G2183 reduces generation of the 1.8-kb RNA in cultured cells (36), it is possible that G3BP may be implicated in alternative upstream cleavages. In fact, the 3′ UTRs of *IGF-II* mRNAs exhibit a conserved polymorphic CA repeat sequence. In agreement with this, we found that *IGF-II* decayed more rapidly in wild-type MEFs than in *G3BP*$^{-/-}$ MEFs (Fig. 6B). Moreover, G3BP is able to bind and cleave the 3′ UTR of *IGF-II* mRNA at available CA sites in vitro (Fig. 6A). Careful analysis of Northern blots using different probes clearly identified a 1.8-kb RNA species corresponding to the product of endonucleolytic cleavage at a specific site in the 3′ UTR of full-length *IGF-II* mRNA (35) in both wild-type and G3BP$^{-/-}$ cells and embryos (data not shown). Loss of G3BP did not abolish the production of this 1.8-kb RNA species, as would have been expected if G3BP is the endoribonuclease that cleaves the long 3′ UTR of *IGF-II* mRNA. However, we cannot exclude the possibility that there are two types of endonucleolytic cleavage of *IGF-II* mRNA, one constitutive and independent of G3BP and the other strictly dependent on G3BP. Constitutive cleavage was previously shown not to contribute to *IGF-II* mRNA stability (60, 61), whereas endonucleolytic cleavage regulated in a cell density-dependent manner does (31). At high cell density, there is an up-regulation of the cleavage of full-length mRNAs (60, 61). In this respect, it is important to recall that G3BP activity itself is modulated by the Ras signaling pathway (21, 59), and the G3BP-mediated endonucleolytic cleavage of *IGF-II* mRNAs could allow a response to exogenous stimuli. Failure to observe an increase of the 1.8-kb RNA cleavage species in G3BP$^{-/-}$ cells while they appear arrested (Fig. 4) is consistent with the possibility that G3BP is involved in the regulated cleavage of *IGF-II* mRNAs.

A surprising result from the transcriptional analysis of G3BP-deficient cells is the small number of genes whose expression is significantly altered compared to wild-type cells (Fig. 4). A large number of these misregulated genes (70%), however, encode signaling molecules, providing further support for the involvement of G3BP in regulation of signaling. Whether G3BP endonuclease activity is limited to the regulation of a few genes and/or G3BP is implicated in mechanisms other than controlling mRNA levels of target genes is difficult to answer at present. It is possible that our analysis has missed short-lived mRNAs like c-*myc* mRNA, which was previously shown to be cleaved by G3BP (21, 59). Alternatively, the continued presence of G3BP2, which also mediates c-*myc* cleavage (25), in *G3BP*$^{-/-}$ fibroblasts could also explain our inability to detect misexpression of other endogenous target genes. This would imply that G3BP and G3BP2 have overlapping but not redundant functions, a possibility that can be tested by studying the consequences of combining the mutation of both genes in the same animal. Nevertheless, G3BP could have a strong preference for some specific target that shares common features and/or is implicated in shared pathways. Growth arrest-specific genes and imprinted genes will fit in both categories. Both types of genes are implicated in processes that regulate cellular growth. In addition, *GAS5* and *IGF-II* mRNAs are non-protein-coding mRNAs or contain long 5′ and 3′ UTRs, respectively, and therefore may escape the major pathways of mRNA decay involving decapping (removal of the cap structure of mRNA) and exonucleolysis (57). Furthermore, *IGF-II* endonucleolytic cleavage does not necessitate active translation but rather requires both a structural RNA determinant and specific growth conditions (49). *GAS1* and *GAS2*, two other growth arrest-specific genes that are up-regulated in the absence of G3BP (Fig. 4C), also have large 5′ UTRs (400 nucleotides [nt] and 244 nt, respectively) and 3′ UTRs (roughly 1,000 nt). It is therefore tempting to speculate that *GAS1*, *GAS2*, and *GAS5* mRNAs might have structural features in common with *IGF-II* mRNA and thus be subjected to the same type of regulation.

An unsolved question raised by this study concerns the low levels of *GAS5* and *IGF-II* mRNAs observed in G3BP$^{-/-}$ embryos during midgestation (E12.5) and the down-regulation of several genes in MEFs. These observations stand in contrast to the implication of the cleaving activity of G3BP at early stages of development. Like other RNA binding proteins, G3BP is probably implicated in several aspects of posttranscriptional processes, such as mRNA localization, turnover, and translational control. Both posttranslational modification of G3BP and other associated activities, like RNA helicase (62) and the ubiquitin modulator (14, 51), may collectively contribute to a concerted control of expression of target genes during development. Interestingly, while the expression profile of G3BP did not change during development (data not shown), analysis of its phosphorylation status revealed that G3BP was

highly phosphorylated by E12.5 and became hypophosphorylated at later stages (data not shown). Since phosphorylation of G3BP modulates both its cellular localization and its activity, this modification is likely to contribute to different functions of G3BP and would help explain different behaviors of G3BP on target mRNAs during development. Moreover, the effect of G3BP may depend on the coordinate expression of other factors, such as IMP1, whose expression peaks at E12.5 and which binds with high affinity to the upstream border of a CA-rich region in the 3′ UTRs of *IGF-II* mRNAs (39, 40) and to H19 RNA (47).

Our data offer new insights into the physiological importance of G3BP. In contrast to *Drosophila*, where mutants with the *Drosophila* homologue of G3BP, Rasputin, deleted ($Rin^{-/-}$) display defects in photoreceptor recruitment and ommatidial polarity in the eye only (43), the disruption of G3BP in mice has proven that both developmental growth and survival are critically dependent on the G3BP level. The absence of defects of proliferation associated with $Rin^{-/-}$ mutants implies that differences may exist between G3BP and Rin in mediating Ras signaling. While many components of the Ras signaling pathway in *Drosophila* are conserved in mammals, including negative regulation of Ras by RasGAP (GAP1 in *Drosphila*), GAP1 lacks SH3 and could not be shown to interact genetically with Rin. It is not known, therefore, whether Rin participation in Ras signaling in *Drosophila* involves interaction with RasGAP, as is the case in mammals. The developmental success of a fraction of $G3BP^{-/-}$ embryos until birth suggests that G3BP is part of a posttranscriptional machinery adapting the cellular response to growth conditions and emphasizes a protective role for neuronal cells during mammalian development. More work should be done with $Rin^{-/-}$ mutants to see if G3BP performs a similar function in *Drosophila*.

ACKNOWLEDGMENTS

We are grateful to Robert Feil and Bob Hipskind for helpful discussions. Special thanks are due to Cécile Dupon and Sophie Maire for technical assistance. We are also grateful to Jean-Michel Itier, Gunter Tremp (SANOFI-Aventis), Chantal Jacquet, and Eric Jouffre of the animal facility at the IGMM for producing transgenic mice.

This work was supported by Centre National de Recherche Scientifique (CNRS), Association pour la Recherche sur le Cancer (ARC), Rhône Poulenc Rorer SA (SANOFI-Aventis), and the Danish Medical Research Council. L.Z. and H.T. were supported by graduate fellowships from the Ligue Contre le Cancer (Comité de l'Herault) and FRM, respectively. To initiate the project, K.C. was supported by fellowships from Rhone Poulenc Rorer SA (SANOFI-Aventis).

REFERENCES

1. **Aronov, S., G. Aranda, L. Behar, and I. Ginzburg.** 2001. Axonal tau mRNA localization coincides with tau protein in living neuronal cells and depends on axonal targeting signal. J. Neurosci. **21:**6577–6587.
2. **Atlas, R., L. Behar, E. Elliott, and I. Ginzburg.** 2004. The insulin-like growth factor mRNA binding-protein IMP-1 and the Ras-regulatory protein G3BP associate with tau mRNA and HuD protein in differentiated P19 neuronal cells. J. Neurochem. **89:**613–626.
3. **Baker, J., J. P. Liu, E. J. Robertson, and A. Efstratiadis.** 1993. Role of insulin-like growth factors in embryonic and postnatal growth. Cell **75:**73–82.
4. **Beelman, C. A., and R. Parker.** 1995. Degradation of mRNA in eukaryotes. Cell **81:**179–183.
5. **Binder, R., J. A. Horowitz, J. P. Basilion, D. M. Koeller, R. D. Klausner, and J. B. Harford.** 1994. Evidence that the pathway of transferrin receptor mRNA degradation involves an endonucleolytic cleavage within the 3′ UTR and does not involve poly(A) tail shortening. EMBO J. **13:**1969–1980.
6. **Binder, R., S. P. Hwang, R. Ratnasabapathy, and D. L. Williams.** 1989. Degradation of apolipoprotein II mRNA occurs via endonucleolytic cleavage at 5′-AAU-3′/5′-UAA-3′ elements in single-stranded loop domains of the 3′-noncoding region. J. Biol. Chem. **264:**16910–16918.
7. **Blichenberg, A., B. Schwanke, M. Rehbein, C. C. Garner, D. Richter, and S. Kindler.** 1999. Identification of a cis-acting dendritic targeting element in MAP2 mRNAs. J. Neurosci. **19:**8818–8829.
8. **Brittis, P. A., Q. Lu, and J. G. Flanagan.** 2002. Axonal protein synthesis provides a mechanism for localized regulation at an intermediate target. Cell **110:**223–235.
9. **Brown, B. D., and R. M. Harland.** 1990. Endonucleolytic cleavage of a maternal homeo box mRNA in *Xenopus* oocytes. Genes Dev. **4:**1925–1935.
10. **Brown, B. D., I. D. Zipkin, and R. M. Harland.** 1993. Sequence-specific endonucleolytic cleavage and protection of mRNA in *Xenopus* and *Drosophila*. Genes Dev. **7:**1620–1631.
11. **Cande, C., N. Vahsen, D. Metivier, H. Tourriere, K. Chebli, C. Garrido, J. Tazi, and G. Kroemer.** 2004. Regulation of cytoplasmic stress granules by apoptosis-inducing factor. J. Cell Sci. **117:**4461–4468.
12. **Christians, E. S.** 2003. When the mother further impacts the destiny of her offspring: maternal effect mutations. Med. Sci. (Paris) **19:**459–464.
13. **Coccia, E. M., C. Cicala, A. Charlesworth, C. Ciccarelli, G. B. Rossi, L. Philipson, and V. Sorrentino.** 1992. Regulation and expression of a growth arrest-specific gene (*gas5*) during growth, differentiation, and development. Mol. Cell. Biol. **12:**3514–3521.
14. **Cohen, M., F. Stutz, and C. Dargemont.** 2003. Deubiquitination, a new player in Golgi to endoplasmic reticulum retrograde transport. J. Biol. Chem. **278:**51989–51992.
15. **DeChiara, T. M., A. Efstratiadis, and E. J. Robertson.** 1990. A growth-deficiency phenotype in heterozygous mice carrying an insulin-like growth factor II gene disrupted by targeting. Nature **345:**78–80.
16. **DeChiara, T. M., E. J. Robertson, and A. Efstratiadis.** 1991. Parental imprinting of the mouse insulin-like growth factor II gene. Cell **64:**849–859.
17. **Delaval, K., and R. Feil.** 2004. Epigenetic regulation of mammalian genomic imprinting. Curr. Opin. Genet. Dev. **14:**188–195.
18. **Ehretsmann, C. P., A. J. Carpousis, and H. M. Krisch.** 1992. mRNA degradation in procaryotes. FASEB J. **6:**3186–3192.
19. **Feldker, D. E., N. A. Datson, A. H. Veenema, V. Proutski, D. Lathouwers, E. R. De Kloet, and E. Vreugdenhil.** 2003. GeneChip analysis of hippocampal gene expression profiles of short- and long-attack-latency mice: technical and biological implications. J. Neurosci. Res. **74:**701–716.
20. **Fontanier-Razzaq, N., D. N. Harries, S. M. Hay, and W. D. Rees.** 2002. Amino acid deficiency up-regulates specific mRNAs in murine embryonic cells. J. Nutr. **132:**2137–2142.
21. **Gallouzi, I. E., F. Parker, K. Chebli, F. Maurier, E. Labourier, I. Barlat, J. P. Capony, B. Tocque, and J. Tazi.** 1998. A novel phosphorylation-dependent RNase activity of GAP-SH3 binding protein: a potential link between signal transduction and RNA stability. Mol. Cell. Biol. **18:**3956–3965.
22. **Hall, J. G.** 1990. Genomic imprinting: review and relevance to human diseases. Am. J. Hum. Genet. **46:**857–873.
23. **Hirose, T., and J. A. Steitz.** 2001. Position within the host intron is critical for efficient processing of box C/D snoRNAs in mammalian cells. Proc. Natl. Acad. Sci. USA **98:**12914–12919.
24. **Ioannidis, P., L. Mahaira, A. Papadopoulou, M. R. Teixeira, S. Heim, J. A. Andersen, E. Evangelou, U. Dafni, N. Pandis, and T. Trangas.** 2003. CRD-BP: a c-Myc mRNA stabilizing protein with an oncofetal pattern of expression. Anticancer Res. **23:**2179–2183.
25. **Irvine, K., R. Stirling, D. Hume, and D. Kennedy.** 2004. Rasputin, more promiscuous than ever: a review of G3BP. Int. J. Dev. Biol. **48:**1065–1077.
26. **Jaenisch, R., and A. Bird.** 2003. Epigenetic regulation of gene expression: how the genome integrates intrinsic and environmental signals. Nat. Genet. **33**(Suppl.)**:**245–254.
27. **Jin, K., X. O. Mao, M. W. Eshoo, G. del Rio, R. Rao, D. Chen, R. P. Simon, and D. A. Greenberg.** 2002. cDNA microarray analysis of changes in gene expression induced by neuronal hypoxia in vitro. Neurochem. Res. **27:**1105–1112.
28. **Katsafanas, G. C., and B. Moss.** 2004. Vaccinia virus intermediate stage transcription is complemented by Ras-GTPase-activating protein SH3 domain-binding Protein (G3BP) and cytoplasmic activation/proliferation-associated protein (p137) individually or as a heterodimer. J. Biol. Chem. **279:**52210–52217.
29. **Kennedy, D., S. A. Wood, T. Ramsdale, P. P. Tam, K. A. Steiner, and J. S. Mattick.** 1996. Identification of a mouse orthologue of the human ras-GAP-SH3-domain binding protein and structural confirmation that these proteins contain an RNA recognition motif. Biomed. Pept. Proteins Nucleic Acids **2:**93–99.
30. **Kuhl, D., and P. Skehel.** 1998. Dendritic localization of mRNAs. Curr. Opin. Neurobiol. **8:**600–606.
31. **Kutoh, E., J. Schwander, and J. B. Margot.** 1995. Cell-density-dependent modulation of the rat insulin-like-growth-factor-binding protein 2 and its gene. Eur. J. Biochem. **234:**557–562.
32. **Leeds, P., B. T. Kren, J. M. Boylan, N. A. Betz, C. J. Steer, P. A. Gruppuso, and J. Ross.** 1997. Developmental regulation of CRD-BP, an RNA-binding protein that stabilizes c-myc mRNA in vitro. Oncogene **14:**1279–1286.

33. **Li, E.** 2002. Chromatin modification and epigenetic reprogramming in mammalian development. Nat. Rev. Genet. **3:**662–673.
34. **Martin, K. C., M. Barad, and E. R. Kandel.** 2000. Local protein synthesis and its role in synapse-specific plasticity. Curr. Opin. Neurobiol. **10:**587–592.
35. **Meinsma, D., P. E. Holthuizen, J. L. Van den Brande, and J. S. Sussenbach.** 1991. Specific endonucleolytic cleavage of IGF-II mRNAs. Biochem. Biophys. Res. Commun. **179:**1509–1516.
36. **Meinsma, D., W. Scheper, P. E. Holthuizen, J. L. Van den Brande, and J. S. Sussenbach.** 1992. Site-specific cleavage of IGF-II mRNAs requires sequence elements from two distinct regions of the IGF-II gene. Nucleic Acids Res. **20:**5003–5009.
37. **Nielsen, F. C., and J. Christiansen.** 1992. Endonucleolysis in the turnover of insulin-like growth factor II mRNA. J. Biol. Chem. **267:**19404–19411.
38. **Nielsen, F. C., and J. Christiansen.** 1995. Posttranscriptional regulation of insulin-like growth factor II mRNA. Scand. J. Clin. Lab. Investig. Suppl. **220:**37–46.
39. **Nielsen, J., J. Christiansen, J. Lykke-Andersen, A. H. Johnsen, U. M. Wewer, and F. C. Nielsen.** 1999. A family of insulin-like growth factor II mRNA-binding proteins represses translation in late development. Mol. Cell. Biol. **19:**1262–1270.
40. **Nielsen, J., M. A. Kristensen, M. Willemoes, F. C. Nielsen, and J. Christiansen.** 2004. Sequential dimerization of human zipcode-binding protein IMP1 on RNA: a cooperative mechanism providing RNP stability. Nucleic Acids Res. **32:**4368–4376.
41. **Parker, R., and H. Song.** 2004. The enzymes and control of eukaryotic mRNA turnover. Nat. Struct. Mol. Biol. **11:**121–127.
42. **Pastori, R. L., J. E. Moskaitis, and D. R. Schoenberg.** 1991. Estrogen-induced ribonuclease activity in *Xenopus* liver. Biochemistry **30:**10490–10498.
43. **Pazman, C., C. A. Mayes, M. Fanto, S. R. Haynes, and M. Mlodzik.** 2000. Rasputin, the *Drosophila* homologue of the RasGAP SH3 binding protein, functions in ras- and Rho-mediated signaling. Development **127:**1715–1725.
44. **Peltz, S. W., and A. Jacobson.** 1992. mRNA stability: in *trans*-it. Curr. Opin. Cell. Biol. **4:**979–983.
45. **Richter, J. D., and L. J. Lorenz.** 2002. Selective translation of mRNAs at synapses. Curr. Opin. Neurobiol. **12:**300–304.
46. **Rozental, R., M. Srinivas, S. Gokhan, M. Urban, R. Dermietzel, J. A. Kessler, D. C. Spray, and M. F. Mehler.** 2000. Temporal expression of neuronal connexins during hippocampal ontogeny. Brain Res. Brain Res. Rev. **32:**57–71.
47. **Runge, S., F. C. Nielsen, J. Nielsen, J. Lykke-Andersen, U. M. Wewer, and J. Christiansen.** 2000. H19 RNA binds four molecules of insulin-like growth factor II mRNA-binding protein. J. Biol. Chem. **275:**29562–29569.
48. **Saini, K. S., I. C. Summerhayes, and P. Thomas.** 1990. Molecular events regulating messenger RNA stability in eukaryotes. Mol. Cell. Biochem. **96:** 15–23.
49. **Scheper, W., D. Meinsma, P. E. Holthuizen, and J. S. Sussenbach.** 1995. Long-range RNA interaction of two sequence elements required for endonucleolytic cleavage of human insulin-like growth factor II mRNAs. Mol. Cell. Biol. **15:**235–245.
50. **Smith, C. M., and J. A. Steitz.** 1998. Classification of gas5 as a multi-small-nucleolar-RNA (snoRNA) host gene and a member of the 5′-terminal oligopyrimidine gene family reveals common features of snoRNA host genes. Mol. Cell. Biol. **18:**6897–6909.
51. **Soncini, C., I. Berdo, and G. Draetta.** 2001. Ras-GAP SH3 domain binding protein (G3BP) is a modulator of USP10, a novel human ubiquitin specific protease. Oncogene **20:**3869–3879.
52. **Steward, O., and E. M. Schuman.** 2003. Compartmentalized synthesis and degradation of proteins in neurons. Neuron **40:**347–359.
53. **Steward, O., and P. F. Worley.** 2001. A cellular mechanism for targeting newly synthesized mRNAs to synaptic sites on dendrites. Proc. Natl. Acad. Sci. USA **98:**7062–7068.
54. **Stewart, C. E., and P. Rotwein.** 1996. Growth, differentiation, and survival: multiple physiological functions for insulin-like growth factors. Physiol. Rev. **76:**1005–1026.
55. **Stoeckle, M. Y.** 1992. Removal of a 3′ non-coding sequence is an initial step in degradation of gro alpha mRNA and is regulated by interleukin-1. Nucleic Acids Res. **20:**1123–1127.
56. **Suyama, M., T. Doerks, I. C. Braun, M. Sattler, E. Izaurralde, and P. Bork.** 2000. Prediction of structural domains of TAP reveals details of its interaction with p15 and nucleoporins. EMBO Rep. **1:**53–58.
57. **Tourriere, H., K. Chebli, and J. Tazi.** 2002. mRNA degradation machines in eukaryotic cells. Biochimie **84:**821–837.
58. **Tourriere, H., K. Chebli, L. Zekri, B. Courselaud, J. M. Blanchard, E. Bertrand, and J. Tazi.** 2003. The RasGAP-associated endoribonuclease G3BP assembles stress granules. J. Cell. Biol. **160:**823–831.
59. **Tourriere, H., I. E. Gallouzi, K. Chebli, J. P. Capony, J. Mouaikel, G. P. van der, and J. Tazi.** 2001. RasGAP-associated endoribonuclease G3Bp: selective RNA degradation and phosphorylation-dependent localization. Mol. Cell. Biol. **21:**7747–7760.
60. **van Dijk, E. L., J. S. Sussenbach, and P. E. Holthuizen.** 2000. Distinct RNA structural domains cooperate to maintain a specific cleavage site in the 3′-UTR of IGF-II mRNAs. J. Mol. Biol. **300:**449–467.
61. **van Dijk, E. L., J. S. Sussenbach, and P. E. Holthuizen.** 2001. Kinetics and regulation of site-specific endonucleolytic cleavage of human IGF-II mRNAs. Nucleic Acids Res. **29:**3477–3486.
62. **Vindigni, A., A. Ochem, G. Triolo, and A. Falaschi.** 2001. Identification of human DNA helicase V with the far upstream element-binding protein. Nucleic Acids Res. **29:**1061–1067.
63. **Wang, Z., and M. Kiledjian.** 2000. The poly(A)-binding protein and an mRNA stability protein jointly regulate an endoribonuclease activity. Mol. Cell. Biol. **20:**6334–6341.
64. **Wilson, G. M., and G. Brewer.** 1999. Identification and characterization of proteins binding A + U-rich elements. Methods **17:**74–83.
65. **Wilusz, C. J., and J. Wilusz.** 2004. Bringing the role of mRNA decay in the control of gene expression into focus. Trends Genet. **20:**491–497.